International Journal of Nanomedicine

Dovepress
open access to scientific and medical research

Open Access Full Text Article

ORIGINAL RESEARCH

Folate-Mediated Targeted Delivery of siPLK1 by Leucine-Bearing Polyethylenimine

This article was published in the following Dove Press journal:
International Journal of Nanomedicine

Lu Hou[1,2]
Zheyu Song[3]
Zhonghang Xu[3]
Yuanyu Wu[3]
Wei Shi[1,2]

[1]College of Life Science, Jilin University, Changchun, Jilin 130012, People's Republic of China; [2]Key Laboratory for Molecular Enzymology and Engineering, Ministry of Education, Jilin University, Changchun 130012, People's Republic of China; [3]Department of Gastrointestinal Colorectal and Anal Surgery, China-Japan Union Hospital, Jilin University, Changchun 130033, People's Republic of China

Background: siRNA-mediated polo-like kinase 1 (PLK1) silencing has been proposed as a promising therapeutic method for multiple cancers. However, the clinic application of this method is still hindered by the low specific delivery of siPLK1 to desired tumor lesions. Herein, folate (FA)-modified and leucine-bearing polyethylenimine was successfully synthesized and showed excellent targeted silencing to folate receptor overexpressed cells.

Materials and Methods: The condensation of siPLK1 by FA-N-Ac-L-Leu-PEI (NPF) was detected by the gel retardation assay. The targeted and silencing efficiency was evaluated by flow cytometry and confocal laser scanning microscope. The PLK1 expressions at gene or protein levels were detected by quantitative real-time PCR and Western blotting assay. Further impacts of the PLK1 silencing on cell viability, cell cycle, migration, and invasion were studied by MTT, colony formation, wound healing and transwell assays.

Results: The NPF and siPLK1 could efficiently assemble to stable nanoparticles at a weight ratio of 3.0 and showed excellent condensation and protection effect. Owing to the FA-mediated targeted delivery, the uptake and silencing efficiency of NPF/siPLK1 to SGC-7901 cells was higher than that without FA modification. Moreover, NPF-mediated PLK1 silencing showed significant anti-tumor activity in vitro. The anti-proliferation effect of PLK1 silencing was induced via the mitochondrial-dependent apoptosis pathway with the cell cycle arrest of 45% at G2 phase and the apoptotic ratio of 28.3%.

Conclusion: FA-N-Ac-L-Leu-PEI (NPF) could generate targeted delivery siPLK1 to FA receptor overexpressed cells and dramatically downregulate the expression of PLK1 expression.

Keywords: targeted delivery, folate, leucine-bearing PEI, siPLK1, gene therapy

Introduction

Overexpression of polo-like kinase 1 (PLK1) is observed in various types of cancers with a positive correlation with the survival of patients.[1] Therefore, PLK1 has been proposed as a promising therapeutic marker for cancer therapy.[2] PLK1 gene silencing by small interfering RNA (siPLK1) dramatically induces the apoptosis of multiple cancer lines in vitro.[3,4] Different delivery systems, such as virus, exosomes, liposomes, polymers, and mesoporous silica nanoparticles, have been applied in the transfection of siPLK1.[5–9] However, in vivo application of siPLK1 is still hindered by low-targeted ability to primary and metastatic tumor regions.[2] As a result, the targeted delivery of siPLK1 has been an emergent challenge for the clinical outcomes of PLK1 depleting therapy.

Folate (FA), as the most popular targeted ligand, has been broadly investigated in drug and gene delivery.[10] FA-decorated nanocomplexes or nanoparticles can selectively bind to the FA receptor overexpressed in the majority of human cancers.[11] Based on the

Correspondence: Wei Shi
Key Laboratory for Molecular Enzymology and Engineering of Ministry of Education, School of Life Sciences, Jilin University, Changchun 130012, People's Republic of China
Tel +86-431-85155216
Fax +86-431-85155200
Email shiw@jlu.edu.cn

submit your manuscript | www.dovepress.com
DovePress
http://doi.org/10.2147/IJN.S227289

specific recognition, modification of FA has been proved to enhance in vitro and in vivo silencing of siRNA to FA receptor-overexpressed cell lines.[12–14] Moreover, PLK1 silencing therapy and FA-mediated targeted are both effective to a broad spectrum of tumor types.[3] Therefore, targeted delivery of siPLK1 via modification of FA might be a promising strategy to enhance the therapeutic effects of PLK1 silencing therapy.

Apart from the active targeted mediated by FA, the optimal vectors for delivery are also important to the effect of delivery. Amino acids-bearing PEIs (aaPEI)s are optimized cationic polymer gene carriers, which exhibit higher transfection effect and lower cytotoxicity compared with PEI.[15–18] Modification of hydrophobic amino acids, including leucine, polyphenylalanine, and poly(γ-benzyl-L-glutamate) (PBLG) segments, decreases the positive charge density of PEI and stabilizes the complexes. Moreover, the shrinkage of size may also promote the endocytosis by targeted cells.[19] The hydrophobic amino acids-bearing PEIs have been proved to greatly improve gene delivery both in vitro and in vivo.[20] However, their application in either targeted delivery or siPLK1 therapy is rarely reported. Based on the benefits of aaPEI, the FA-functionalized ones might be a candidate with great potential in targeted delivery.

Herein, we reported an FA-modified leucine-bearing PEI (NPF) for efficient targeted delivery of siPLK1 to FA receptor-overexpressed human gastric cancer (SGC-7901) cell line in vitro. Additionally, the leucine-bearing PEI (NP) without FA modification was also synthesized as a control. The cationic polymer was prepared by conjugation of FA-premodified N-acetyl-leucine to PEI. With the contribution of FA-mediated targeted ability, the siPLK1-loaded NPF (NPF/siPLK1) could obtain better cellular uptake to FA-overexpressed cell lines, which would further promote the gene-silencing effect of siPLK1. Such a design might be a candidate route to improve the targeted delivery and therapeutic effect of siPLK1.

Materials and Methods

Materials

Branched polyethylenimine with a weight-average molecular weight of 25 kDa (PEI25K), bovine serum albumin (BSA), and trypsin were purchased from Sigma-Aldrich corporation (Shanghai, China). N-Acetyl-L-leucine (N-Ac-L-Leu), N-hydroxysuccinimide (NHS), folic acid (FA), and 1-(3-dimethylaminopropyl)-3-ethylcarbodiimide hydrochloride (EDC•HCl) were bought from Aladdin (Shanghai, China). Methylthiazolyldiphenyl-tetrazolium bromide (MTT) and 4′,6-diamidino-2-phenylindole (DAPI) were obtained from Amresco, Inc (OH, USA). Anti pro-caspase-3, anti-caspase-8, anti-caspase-9, anti-notch-1, anti-β-actin, HRP-labelled goat anti-rabbit IgG, and HRP-labelled goat anti-mouse IgG were all purchased from Abcam (Shanghai, China). BCA protein quantification kit was bought from Dingguo Co. (Beijing, China). AnnexinV-FITC/PI apoptosis detection kit and cell cycle detection kit were purchased from Bestbio (Shanghai, China). Polyvinylidene fluoride (PVDF) membrane was purchased from Millipore (NH, USA). JC-1 probe mitochondrial membrane potential detection kit, RIPA and protease inhibitor (PMSF) and RNase (10 mg/mL) were purchased from Biyuntian (Shanghai, China). RNA reverse transcription kit and SYBRTM Green real-time qPCR kit were purchased from TAKARA Bio. Inc. (Beijing, China). The protein pre-stained rainbow marker, ECL chromogenic kit, and TranZol UP RNA extraction reagent were purchased from Transgene (Beijing, China). The live/dead viability/cytotoxicity kit was purchased from Invitrogen (NY, USA). high glucose DMEM medium, RPMI-1640 medium, and fetal bovine serum (FBS) were purchased from Gibco (MT, USA). Protein loading buffer was purchased from Bioteke (Beijing, China).

Sequence of siPLK1 and Negative Control siRNA

The siPLK1 and negative control siRNA (NC siRNA) were synthesized by Suzhou GenePharma Co., Ltd. (Suzhou, China). The sequences were listed as follows: siPLK1-501 sense, 5′-GCACCGAAACCGAGUUAUUTT-3′; siPLK1-501 antisense, 5′-AAUAACUCGGUUUCGGUGCTT-3′; NC siRNA sense, 5′-UUCUCCGAACGUGUCACGUTT-3′; NC siRNA antisense, 5′-ACGUGACACGUUCGGAGAATT −3′.

Synthesis of NP and NPF

The leucine-bearing PEI was synthesized through condensation reaction between carboxyl group in N-Ac-L-Leu and amine groups in PEI according to the method described previously (Scheme 1). [21] First, N-Ac-L-Leu (0.28 g, 1.2 mmol) and EDC•HCl (1.15 g, 6 mmol) were dissolved in anhydrous ethanol. After stirring for 1 hr, NHS (0.69 g, 6 mmol) was added into the above solution. After the activated N-Ac-L-Leu were added dropwise into PEI (0.5 g, 0.02 mmol) dissolved in water. The reaction was stirred under room temperature for another 24 h. The

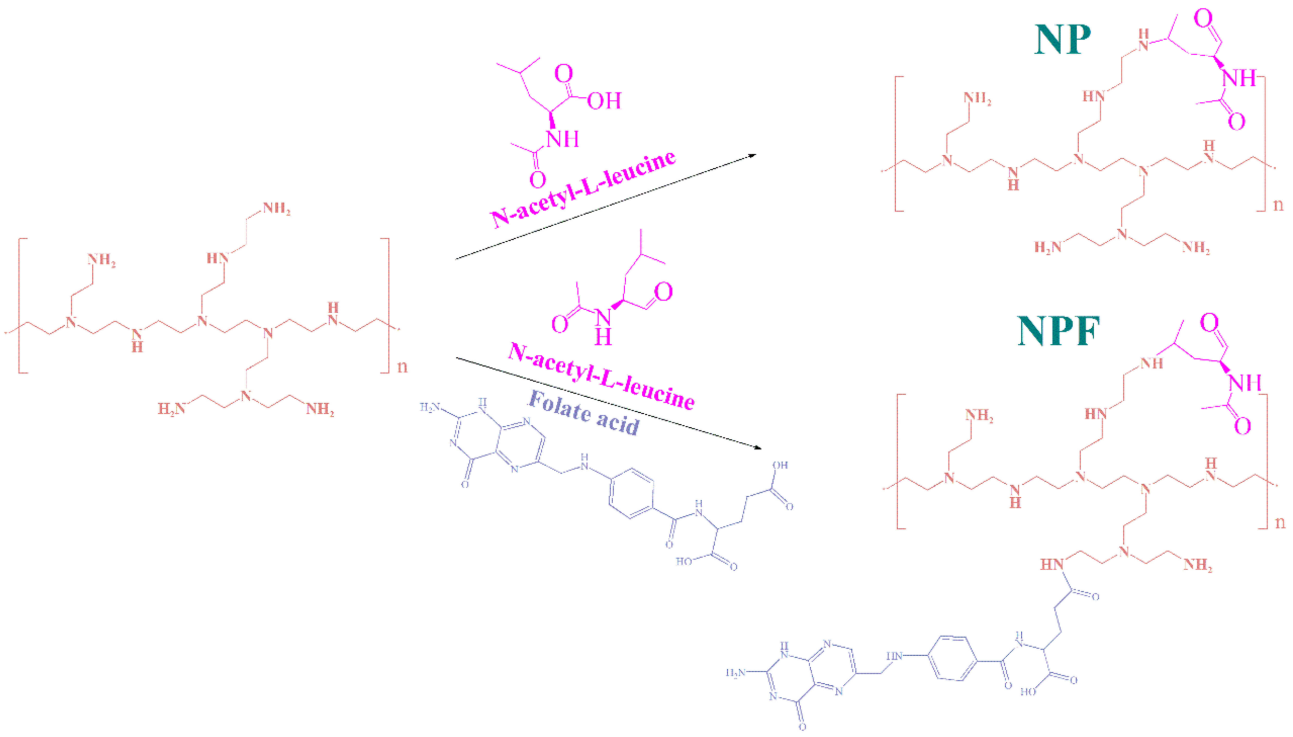

Scheme 1 Synthesis route and chemical structure of NP and NPF.

final product was obtained through dialysis (molecular weight cut-off: 8 ~ 14 KDa) and freeze-drying.

The FA-modified leucine-bearing PEI was synthesized by conjugation of FA and leucine to PEI in one pot. Similarly, N-Ac-L-Leu (0.28 g, 1.2 mmol) and FA (0.26 g, 1.2 mmol) were activated by EDC•HCl (1.15 g, 6 mmol) and NHS (0.69 g, 6 mmol) and then reacted with PEI (0.5 g, 0.02 mmol). The reacted solution was dialyzed and freeze-dried. The NP and NPF were characterized by nuclear magnetic resonance spectroscopy (^{1}H NMR).

Optimization and Characterization of siRNA-Loaded NP and NPF

The condensation ability of PEI, NP and NPF to siRNA was proved and determined by gel retardation assay. PEI was mixed with 0.5 μg of NC siRNA at N/P ratio of 0, 0.7, 1.5, 2.2, 2.9 and 3.6, NP was mixed with 0.5 μg of NC siRNA at N/P ratio of 0, 2, 4, 6, 8, 13, and 16, NPF was mixed with 0.5 μg of NC siRNA at N/P ratio of 0, 2, 3, 5, 7, 10, and 14. Free siRNA was separated from the complex by electrophoresis in 1% agarose gel with ethidium bromide at 120 V for 10 min. The gel was imaged by Bio-rad Universal Hood II (Bio-rad Laboratories, CA, USA).

The protection of siRNA from RNase degradation by NP and NPF was confirmed as reported methods.[22] NP and NPF loaded with NC siRNA at 4:1 (w/w) were incubated with 1 μg/μL RNase at room temperature for 30 min. The siRNA protected in the complex was released from the complex by treatment of 1% SDS solution and then separated by electrophoresis. The gel was also imaged by Bio-rad Universal Hood II.

The diameters of the NC siRNA-loaded NP and NPF at different weight ratios were characterized by Malvern Nano ZS90 Zetasizer (Malvern Panalytical, MA, USA). The further morphology of the NC siRNA-loaded NP and NPF were analyzed by transmission electron microscopy (TEM) at the accelerating voltage of 200 kV. The fourier-transformed infrared spectrometry (FTIR) spectra were recorded in the range of 4000–400 cm^{-1} using KBr pellets on a Bruker V70 FTIR spectrometer. The structure of N-Ac-L-Leu, Folate acid and NPF were characterized by an AVANCE DMX 500 NMR spectrum (Bruker, Rheinstetten, Germany) using D_2O or (Methyl sulfoxide)-d6 as the solvent.

Cell Culture

FA-overexpressed human gastric cancer cell line (SGC-7901) and FA-normal expressed human lung adenocarcinoma cell line (A549) were purchased from the Shanghai Institute of Cell Bank (Shanghai, China). The cells were incubated in Dulbecco's Modified Eagle Medium

(DMEM) with 10% FBS, 100 U/mL of penicillin, and 100 U/mL of streptomycin (completed DMEM).

General Protocol for siRNA Transfection by NP and NPF

Typical transfection was carried out as follows: First, the cells were cultured with completed DMEM in 6 or 96-well plates for 24 hrs. Second, the medium was removed and cells were washed with PBS twice. Then, the medium was replaced by DMEM without FBS. Third, the NP and NPF were mixed with siRNA for 30 mins and added into each well. After 6 hrs of incubation, the medium was replaced with completed DMEM and the cells were cultured for another 48 hrs before further evaluation.

Evaluation of Targeted Delivery of siRNA by NPF

Flow Cytometry (FCM)

The optimized ratio for transfection was determined through flow cytometry. First, 2×10^5 SGC-7901 or A549 cells were cultured in 6-well plates with FA-free Roswell Park Memorial Institute (RPMI) 1640 basic medium with 10% FBS for 24 hrs. NP or NPF were mixed with 5-carboxyfluorescein (FAM)-labelled NC siRNA (FAM-siRNA) at different weight ratios for 30 mins. Afterwards, the formulated complexes were added into the above medium at a final FAM-siRNA concentration of 100 nM. After 6 hrs of incubation, the cells were collected, detected by FACS Calibur (Becton, Dickinson and Company, NJ, USA), and analyzed by FlowJo.

The FA-mediated targeted ability of NPF was also evaluated by FCM. 2×10^5 SGC-7901 or A549 cells in 6-well plates with or without pretreatment of 1.25 mM FA were transfected by NP or NPF loaded with FAM-siRNA at the optimized ratio of 7.5:1 as described before. After transfection, the cells were collected and detected by FACS Calibur.

Confocal Laser Scanning Microscope (CLSM)

1×10^5 SGC-7901 or A549 cells in 6-well plates with or without pretreatment of FA were transfected with NP or NPF loaded with FAM-siRNA at the weight ratio of 7.5:1 as described before. After transfection, the cells were washed with PBS for three times and then fixed with 75% cold ethanol at 4°C for 20 mins. Then, the cells were washed with PBS for another three times and stained with DAPI for 10 mins. The slides were observed and imaged by Zeiss LSM710 (Carl Zeiss, Jena, Germany).

RNA Isolation and Real-Time Quantitative RT-PCR

The cells treated with different formulations for 48 hrs were lysed by TranZol and total RNA was extracted according to the manufacturer's instruction. Reverse transcription (RT) was executed by Prime Script RT Master Mix (TAKARA) with 1μg total RNA. The resulting complementary DNA was quantitated by qPCR on ABI 7500 Real Time PCR System (Invitrogen). PLK1 mRNA levels were normalized to β-Actin mRNA levels. The RT primers were designed as follows: PLK1 sense, 5′-CCCCTCACAGTCCTCAATAA -3′; PLK1 antisense, 5′-TGTCCGAATAGTCCACCCA-3′; β-Actin sense, 5′-GGATCAGCAAGCAGGAGTATG-3′; β-Actin antisense, 5′-CACCTTCACCGTTCCAGTTT-3′.

Protein Isolation and Western Blot

The cells treated with different formulations for 48 h were washed twice by PBS and then collected using 0.25% trypsin. The cells were washed by PBS again and incubated with radioimmunoprecipitation assay (RIPA) buffer with 1 mM PMSF. The total protein concentration was analyzed by BCA method according to the manufacturer's instruction. The denatured proteins were separated by SDS-PAGE using 4–12% polyacrylamide gel and then transferred to PVDF membrane. After blocking with 10% non-fat milk, the PVDF membrane was incubated with primary antibody at 4°C overnight. The PVDF membrane was washed by PBS with 0.1% tween 20 (PBST) three times and then incubated with corresponding secondary antibody for 1 hr at room temperature. Finally, the membrane was washed by PBST for another three times and then detected by enhanced chemiluminescence (ECL).

MTT Assay

7×10^3 SGC-7901 or A549 cells in 96-well plate were transfected by different formulations at the siRNA concentration of 100 nM as described before. After transfection, the cells were treated by 20 μL of MTT solution at 5 mg/mL for another 4 hrs. Finally, the medium was removed and 100 μL of DMSO was added into the well. The optical density (OD) values of each well at 492 nm were detected by plate reader. The cell viability was analyzed according to equation 1.

$$\text{Cell viability}(\%) = \left(A_{\text{smaple}} - A_0\right) / \left(A_{\text{UT}} - A_0\right) \times 100\% \quad (1)$$

In equation 1, A_{sample} represents the OD values of wells treated with corresponding formulations. AUT represents the OD values of wells without treatment. A_0 represents blank plates.

Cell Cycle and Apoptosis Assay

2×10^5 SGC-7901 cells in 6-well plates were transfected with NP or NPF loaded with 100 nM siPLK1 at a weight ratio of 7.5:1. Blank or NC siRNA-loaded NPF and PEI/siPLK1 were used as negative and positive control, respectively.

For cell cycle assay, the cells were collected and washed by PBS. Then, the cells were fixed with 70% ethanol at 4°C overnight. After washing with PBS for another three times, the cells were resuspended with 200 μL PBS containing 20 uL RNase A. After incubated at 37°C for 30 mins, the cells were stained with PI for 30 mins and detected by FCM. DNA histogram analysis was performed using ModFit 5.0 (Verity Software, Topsham, ME).

For cell apoptosis assay, the cells were collected and stained with AnnexinV-FITC/PI apoptosis detection kit according to the manufacturer's instruction. After staining, the cells were detected by FCAS Calibur and analyzed by FlowJo.

Colony Formation Assay

2×10^5 SGC-7901 cells in 6-well plates were transfected with NP or NPF loaded with 100 nM siPLK1 at a weight ratio of 7.5:1. Blank or NC siRNA-loaded NPF and PEI/siPLK1 were used as negative and positive control, respectively. After transfection, the cells were collected and re-culture to new 6-well plates at the concentration of 1×10^4 per well for another 7 days. Then, the cells were washed by PBS and fixed by 70% ethanol at 4°C for 20 mins. Finally, the cells were stained with 0.1% crystal violet staining solution and observed by inverted microscope.

Cell Migration and Invasion

A well-established wound-healing assay was applied for evaluation of cell migration after PLK1 silence. 2×10^5 SGC-7901 cells were cultured in 6-well plate and proliferated up to 95% convergence. A scratch on the bottom of the well was generated by 200 uL tips. Then, the cells were transfected by NP or NPF loaded with 100 nM siPLK1 at a weight ratio of 7.5:1. Blank or NC siRNA-loaded NPF and PEI/siPLK1 were used as negative and positive control, respectively. Images of the wounds were imaged at 0, 12, 24, 36, and 48 hrs after replacement of the medium and the length of the wounds were recorded. The cell migration ability was calculated by equation 2.

$$\text{Migration rate}(\%) = (W_t - W_0)/W_0 \times 100\% \quad (2)$$

In equation 2, W_t and W_0 represented the width of the wound at t h and 0 h, respectively.

Results and Discussion

Preparation and Characterization of NPF

The successful conjugation of L-leucine and FA was proved by ^{1}H NMR. We further calculated the graft ratio of leucine and FA through the peak area of the typical chemical shifts as shown in Figure S1B. In detail, each PEI25K has 581 repeat segments -(CH_2CH_2NH)- and 2325 hydrogen atoms. There are two typical peaks marked as a and b in FA. Each Leu has six typical peaks which were marked as d. The numbers of Leu per PEI25K were determined to be 81 according to the ratio of the peak areas of b and hydrogen in PEI25k. The numbers of FA per PEI25K were also calculated to be 16 through a similar way. FTIR was conducted to further verify the structure of NP and NPF, as shown in Figure S2, the absorption at 1733 cm^{-1} was assigned to the C=O bond in Leu, which confirmed the conjugation of Leu to PEI. Moreover, the absorption at 1605 cm^{-1} of NPF represents the C=N bond in FA, which further proved the successful modification of FA to PEI. GPC has also been conducted, the elution time of NP and NPF was 15.421 and 15.408 min, respectively. The increased molecule also indicated the conjugation of FA to PEI.

As shown in Figure S3, PEI showed great condensation ability when the N/P ratio of PEI to NC siRNA increased to 2.9 or higher. Compared with PEI, the binding ability of NP and NPF to nucleic acids decreased owing to the reduced numbers of positive amine groups after the reaction with folic acid and N-Ac-Leu. Only when the N/P increased to about 10, the siRNA could be totally condensed by NP and NPF (Figure 1A). Additionally, as shown in Figure 1B, siRNA encapsulated into both NP and NPF could be protected from the degradation of RNase, while free siRNA was totally degraded under the same condition. All the results revealed the modified PEI also showed excellent condensation and protection of siRNA. Even though the modification decreased the efficiency of PEI, the toxicity of NP and NPF to both HEK293 and SGC-7901 cells were significantly reduced, and especially in the normal HEK293T cell line. As shown in Figure S4, the unmodified PEI showed significant toxicity to both normal and tumor cell lines. However, the toxicity of NP and NPF reduced after the modification in tumor cells. Even at a concentration of 80 ng/μL,

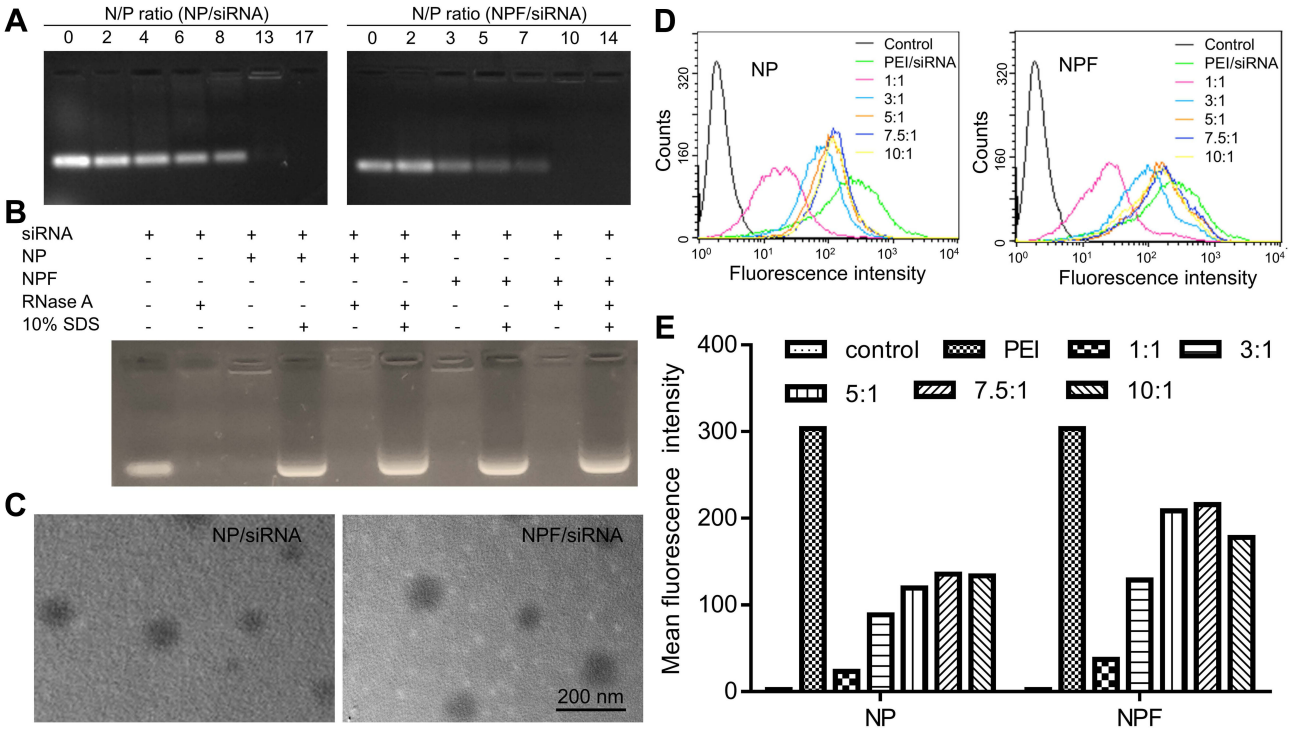

Figure 1 (**A**) The condensation of NC siRNA by NP and NPF at different N/P ratios; (**B**) Protection of NC siRNA from the degradation of RNase by NP and NPF; (**C**) Typical TEM images of NP and NPF loaded with NC siRNA at the weight ratio of 7.5:1. (**D**) FCM analysis of SGC-7901 cells incubated with FAM-siRNA loaded NP and NPF. (**E**) Mean fluorescence intensity calculated by FCM data in Figure 1D.

Abbreviations: NP, N-acetyl-L-leucine-polyethylenimine; NPF, Folate-N-acetyl-L-leucine-polyethylenimine; N/P ratio, the ratio of positively chargeable polymer amine (N = nitrogen) groups to negatively charged nucleic acid phosphate (P) groups.

approximately 50% cell viability could still be observed in NP/NPF treated SGC cell cells. This phenomenon indicated that compared with PEI, NP and NPF have lower cytotoxicity, especially in normal cells. Therefore, the modified PEIs have the broader potential of medical application. In the previous study, we have found NP has the advantage of p53 plasmid transfection.[23] Therefore, the transfection of EGFP plasmid by NP and NPF was conducted and demonstrated that compared with PEI/pEGFP (weight ratio=2:1), the efficiency of pEGFP transfection by NP and NPF was much higher and increased with weight ratio (0.8–8) (Figure S5), which is due to the modification of N-Ac-L-Leu. Based on this, the ability of siRNA transfection was further explored. To optimize the delivery condition of our nanoparticles, series of nanocomplexes with different weight ratios were prepared and characterized in Table S1. The zeta potential of these nanocomplexes increased along with the increasing of weight ratio, suggesting the binding of negatively charged siRNA to positively charged nanoparticles. The sizes of the siRNA-loaded NP and NPF were all in the range of 200 to 270 nm, showing the trend of decrease when the weight ratio increased. Meanwhile, the distributions of these nanocomplexes at higher weight ratio were much broader than those in lower weight ratio, which might result from that the increasing of zeta potential made nanocomplexes more stable and less aggregation. Moreover, the typical morphologies of NC siRNA-encapsulated NP and NPF at the weight ratio of 7.5:1 were captured by TEM in Figure 1C. Both the two nanocomplexes exhibited a spherical structure. The optimized weight ratio of NP and NPF to siPLK1 were determined to be 7.5:1 (N/P ratio is 31.37 and 25.73, respectively) by the cellular uptake of FAM-siRNA to SGC-7901 cells (Figure 1D and E). Therefore, the following experiments in this paper were conducted at this weight ratio.

Targeted Internalization of NPF Mediated by FA Modification

In order to prove the targeted ability after modification of FA, the internalization of FAM-labelled siRNA (FAM-siRNA) to SGC-7901 (FA overexpressed) and A549 (FA normal expressed) mediated by NPF and NP were measured through FCM and CLSM.

The targeted ability of NPF was first evaluated by FCM. As shown in Figure 2A and B, the FAM-siRNA encapsulated NPF exhibited stronger intensity of green

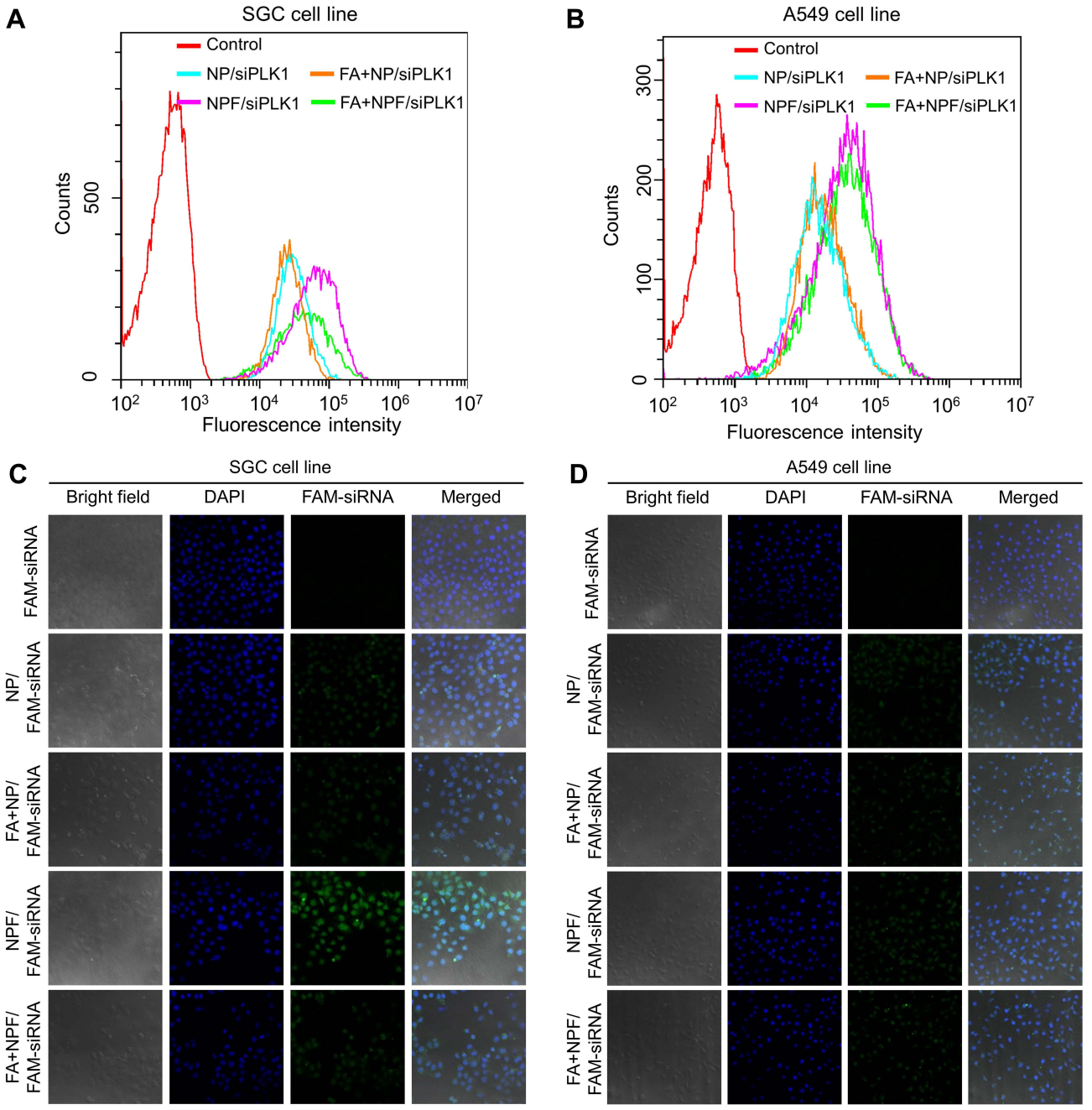

Figure 2 (**A** and **B**) Cell uptake of FAM-siRNA to SGC-7901 (**A**) or A549 (**B**) cells mediated by NP or NPF measured by FCM. (**C** and **D**) Intracellular distribution of FAM-siRNA to SGC-7901 (**C**) or A549 (**D**) cells mediated by NP or NPF captured by CLSM. FA represented the cells pretreated with free FA to block the FA receptor on cell membrane.
Notes: Blue, DAPI; Green, FAM-labeled siPLK1. The scale bar is 50 μm.
Abbreviations: NP, N-acetyl- L-leucine-polyethylenimine; NPF, Folate- N-acetyl- L-leucine-polyethylenimine; FA, folate; FAM, 5-Carboxyfluorescein.

fluorescence compared with NP, indicating the modification of FA did promote the endocytosis of NPF. Additionally, the blocking of FA receptor by free FA decreased the fluorescent intensity in the NPF group, while showing no difference in the NP treated cells. Such reduced internalization further proved the enhanced cellular uptake of NPF was mediated by FA modification. In contrast, for A549 cells, only a slight increase in the green signal in the NPF group compared with that in the NP group could be observed, revealing the normally expressed FA receptor could not benefit the internalization of NPF. Furthermore, such difference of internalization between SGC-7901 and A549 cells proved the targeted ability of NPF to FA-overexpressed cells. The promoted cellular uptake mediated by FA was also proved by CLSM in Figure 2C and D. SGC-7901 cells exhibited the

strongest green fluorescence of FAM-siRNA in NPF groups compared with those in other groups. Similarly, pretreatment of FA dramatically inhibited the green signal in SGC-7901 cells due to the blocking of the FA receptor. Moreover, the significant enhancement of FAM signal did not appear in A549 cells, which was consistent with the results measured by FACS. The promoted internalization was mediated by the overexpression of the FA receptor in SGC-7901 cells, revealing the good targeted ability of NPF after FA modification. Meanwhile, the normal expression of the FA receptor in A549 cells did not cause off-targeted effect, which ensured the safety of normal tissues. In addition, the targeted ability mediated by the FA receptor was further proved by a fluorescence microscope. As shown in Figure S6, compared with NP, Cy3-siRNA encapsulated NPF showed the stronger intensity of red fluorescence in non-labeled SGC-7901 cells. After blocking of FA receptor by free FA, the red fluorescent in the NPF group obviously decreased in non-labeled SGC-7901 but not in the NP group. However, in green fluorescent labeled A549 cells, there was no obvious change in the intensity of Cy-3-siRNA in both NP and NPF groups with or without blocking of the FA receptor, which is due to the modification of folate acid provided targeted ability of NPF to cells overexpressed FA receptor.

Cell Apoptosis and Proliferation Inhibition by Targeted Delivery of siPLK1

Since NPF/siPLK1 showed good targeted effect to FA overexpressed cells, we conducted cellular experiments to detect the silencing and therapeutic effect on SGC-7901 cells. First of all, three different siPLK1 targeted different sequences of PLK1 mRNA were designed for PLK1 silencing, noted as 420, 501, and 671. The most effective siPLK1 was chosen by a simple screening of the silencing effect by PEI in Figure S7.

PLK1 was proved to be an early trigger for G2/M transition, which supported the functional maturation of the centrosome in late G2/early prophase and the establishment of the bipolar spindle.[24] Therefore, inhibition of PLK1 should exhibit the obvious cell cycle arrest in G2 phase. As shown in Figure 3A and B, the treatment of NP/siPLK1 for 6 hrs did not show significant arrest in the G2 phase of SGC-7901 cells compared with the control group. However, the cells incubation with NPF/siPLK1 arrested about 45% of cells in G2 phase, resulting from the depletion of PLK1. The enhanced cell cycle arrest mediated by NPF/siPLK1 compared with that of NP/siPLK1 might result from FA-triggered targeted delivery of siPLK1 to SGC-7901 cells.

The increased cell cycle arrest caused by NPF/siPLK1 led to enhanced cell apoptosis. As shown in Figure 3C, the control SGC-7901 cells showed few apoptotic cells, while the treatment of NPF/NC or blank NPF slightly increased the number of apoptotic cells to 14.4% and 15.8%, respectively. Moreover, NP/siPLK1 only induced a modest apoptosis effect (about 19.1%) without the help of FA modification. However, after the treatment of NPF/siPLK1, the apoptotic rate increased to 28.3%, contributing to the facilitated targeted delivery of siPLK1 to SGC-7901 cells.

Further MTT assay in Figure 3D showed the NPF/siPLK1 could inhibit the cell proliferation of SGC-7901 to about 65%, while the cells treated with blank NPF still had high viability above 80%. The inhibition of cell proliferation also confirmed by live/dead staining in Figure S8. After incubation by different formulations, live cells were stained to green by calcein AM and dead cells were stained to red by ethidium homodimer-1. By calculating the ratio of red to green cells, the cells treated with NP/siPLK1 and NPF/siPLK1 both showed increased numbers of red signal representing dead cells. Moreover, the red signal in the NPF/siPLK1 treated group was slightly higher than that in the NP/siPLK1 group, revealing the targeted delivery efficiency mediated by FA modification. However, in the blank NPF or NPF/siPLK1 treated group, the cells all seemed to be green without any death.

Targeted PLK1 Silencing of NPF/siPLK1 Induced Endogenous Apoptosis Pathway

To evaluate the interruption of PLK1 mRNA by siPLK1 silencing, RT-qPCR were applied to obtain a convincing conclusion in Figure 4A. Blank NPF or NPF loaded with control siRNA did not show the dramatical effect on the PLK1 mRNA level in SGC-7901 cells, while both the siPLK1-encapsulated NP and NPF exhibited obvious PLK1 mRNA inhibition to some extent. Moreover, the PLK1 mRNA level in NPF/siPLK1 group (about 26.5%) was significantly lower than that in NP/siPLK1 group (about 62.3%), confirming the better silencing behavior of NPF/siPLK1 mediated by FA modification. Further analysis of protein expression was also carried out to prove the targeted silencing effect of NPF in protein level. As the effective depletion of PLK1 mRNA in the NPF/siPLK1 group, the PLK1 protein also decreased in these groups.

The depletion of PLK1 protein further affected multiple cell signal pathways and induced cell apoptosis, which was

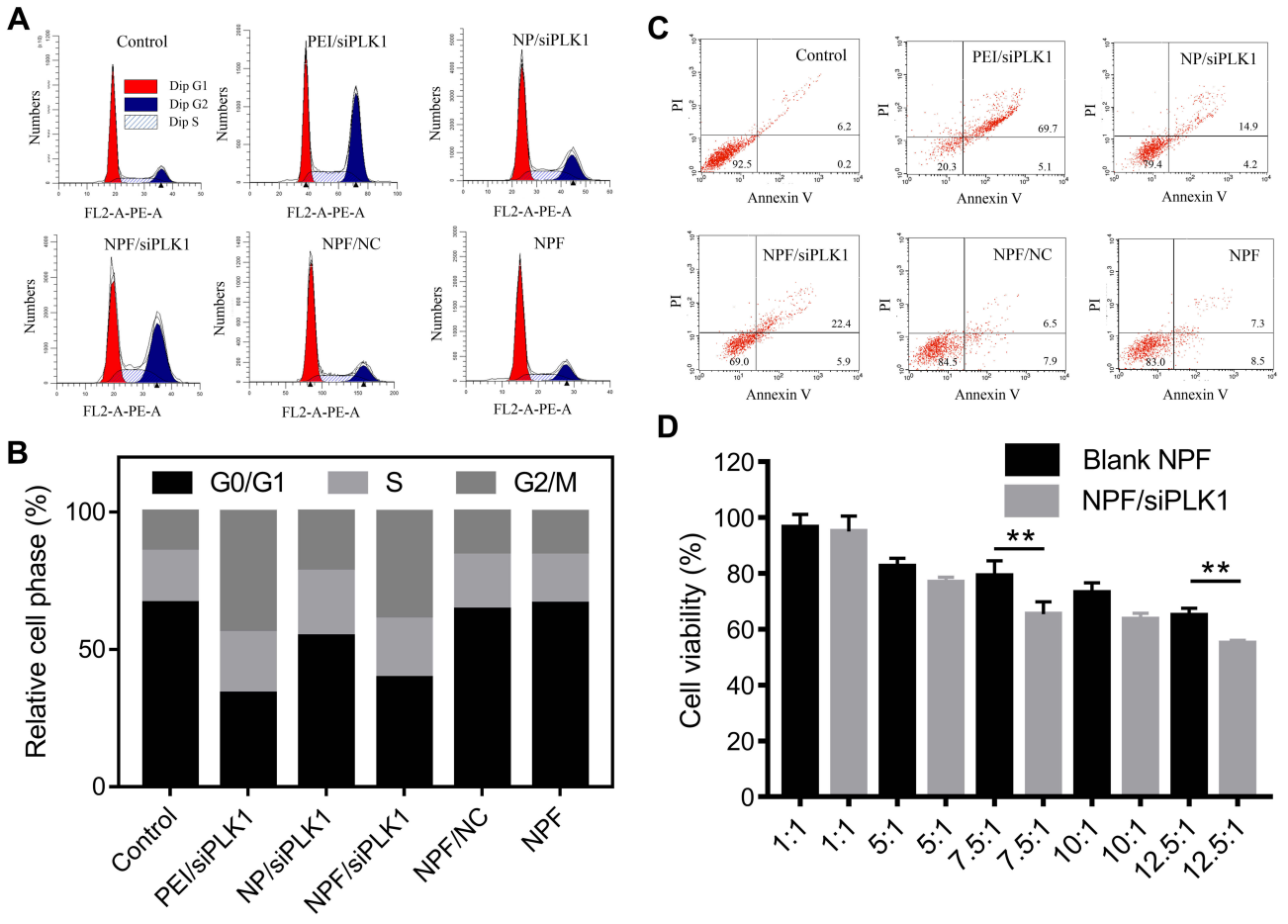

Figure 3 (**A**) DNA histograms of SGC-7901 cells transfected by different complexes. (**B**) Percentage of cell phase calculated from DNA histograms. (**C**) FCM analysis of transfected SGC-7901 cells stained with Annexin V/PI. (**D**) Cell viability of transfected SGC-7901 cells at different weight ratios by MTT assay.
Notes: The data were presented as the mean ± SD of quintuplicate experiments, $^{**}P<0.01$
Abbreviations: NP, N-acetyl- L-leucine-polyethylenimine; NPF, Folate- N-acetyl- L-leucine-polyethylenimine.

broadly reported by previous works. This was consistent with the result shown in Figure 3. Wu et al found knockdown of PLK1 inhibited autophagy in glioma cells, and the inhibition of autophagy induces tumor cell apoptosis. Meanwhile, apoptosis signaling-related proteins: cleaved caspase-3 was significantly elevated while the anti-apoptotic protein Bcl-2 was significantly downregulated in shPLK1-infected U251 cells;[25] Yonghuan Mao et al demonstrated that Plk1 inhibition can lead to cancer cell apoptosis through inactivating XIAP, activating caspase-3, upregulating BAX and downregulating Bcl-2;[26] Noboru Sekimoto et al have researched that KPNB1 expression was decreased by PLK1 inhibition. It is possible that KPNB1 depletion plays a part in the apoptosis observed in PLK1-depleted cells.[27]

To figure out the exact apoptosis pathway caused by the silencing of our nanocomplexes, the expressions of multiple apoptosis-related proteins were also detected by Western blot. The caspases 3 and 9 were two downstream apoptosis-related proteins within the endogenous mitochondrial death pathway, which were activated by the cleavage of pro-caspase 3 and 9 proteins, respectively.[28] In Figure 4B, significant degradation of pro-caspase 3 and 9 proteins in SGC-7901 cells could be observed after 6 hrs of treatment by siPLK1-encapsulated NP and NPF. Furthermore, the activated caspase 3 induced the cleavage of the PRAP involved in DNA repair in response to environmental stress, which facilitated cellular disassembly and served as a marker of apoptosis.[29] However, the expression of caspase 8 protein, a downstream signal of multiple exogenous death regulators, showed no obvious changes in all groups, revealing the activation of caspase 3 and 9 were mediated by the endogenous mitochondrial death. Further detection of mitochondrial membrane potential also confirmed the activation of the mitochondrial death pathway. As shown in Figure S9, the sharp decrease in mitochondrial membrane potential detected by the changes of fluorescence signal from red to green was showed in siPLK1-loaded PEI, NP, and NPF

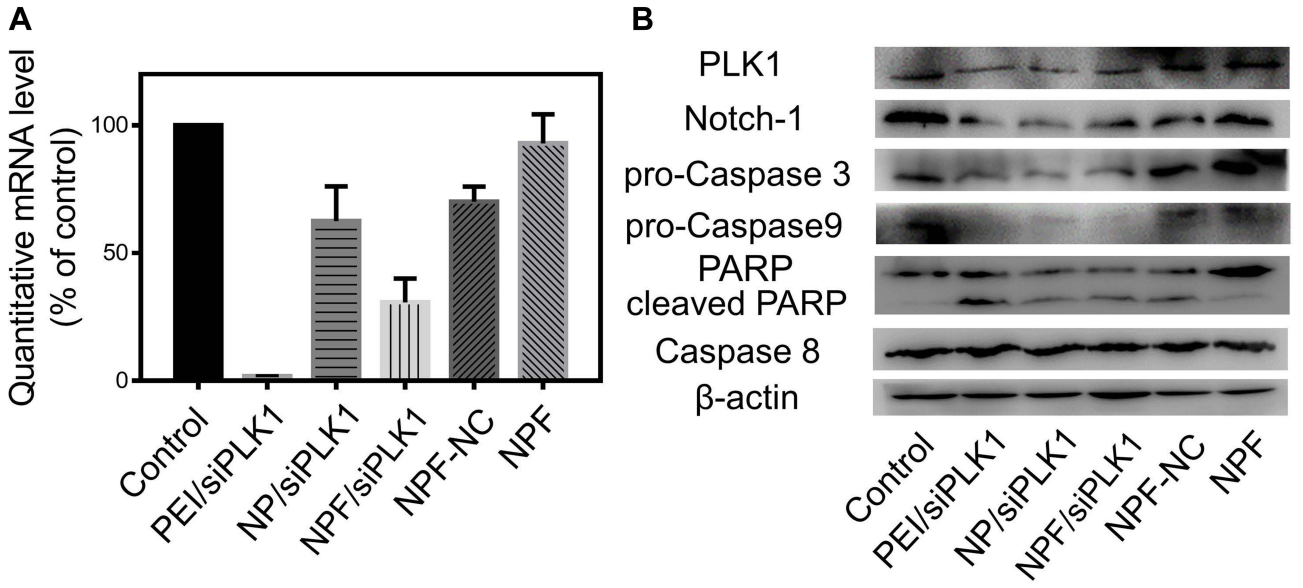

Figure 4 (**A**) Quantitative PLK1 mRNA expression in SGC-7901 cells after transfection by RT-qPCR. (**B**) Expression of PLK1 protein and related proteins in SGC-7901 cells after transfection analysed by Western Blot.
Notes: The data were presented as the mean ± SD of triplicate experiments, $^{**}P<0.01$
Abbreviations: NP, N-acetyl- L-leucine-polyethylenimine; NPF, Folate- N-acetyl- L-leucine-polyethylenimine; RT-qPCR, real-time quantitative PCR.

groups. Moreover, another important cell survival and proliferation-related protein, Notch-1, was also inhibited after the treatment of siPLK1 nanoparticles.[30] The activation of the mitochondrial death pathway by siPLK1 delivery suggested the predicable ability of proliferation inhibition of siPLK1-encapsulated nanoparticles.

NPF/siPLK1 Generated Inhibition of Colony Formation, Cell Migration and Invasion

The influence of these nanocomplexes on multiple cell behaviors, such as colony formation, cell migration and invasion, were also evaluated to further prove the anticancer potential of NPF/siPLK1 to FA-overexpressed cell lines.

The ability to form a cell colony was an important indicator of in vitro cell survival based on the ability of single cell to grow into a cell colony.[31] Different from cell proliferation assay, this method essentially evaluated if every cell in the population had the ability to undergo unlimited division. In Figure 5A, the treatment of siPLK1-loaded nanoformulations all showed good inhibition of the colony formation. Additionally, colony numbers in NPF/siPLK1 treated group decreased more obviously than that treated by NP/siPLK1. The upregulated inhibition effect might be attributed to the enhanced PLK1 silencing mediated by FA-promoted targeted delivery.

The great capability of migration and invasion are two essential features of highly metastatic cancer cells.[32] As a result, the inhibition of these two cell behaviors might reduce the metastasis of cancer cells. A wound-healing assay was applied to evaluate the ability of migration of the SGC-7901 cells after PLK1 silencing in Figure 5B. The cell migration ability was evaluated by the ratio of the final to the initial width of the wound. As the time increased from 0 to 48 h, the wound area recovered rapidly and nearly disappeared in control, NPF/NC, and blank NPF group, which represent a strong migration ability of cells. However, as shown in Figure 5C, after the treatment of NPF/siPLK1, the rate of wound healing decreased significantly with a final wound ratio of about 55%. Compared to it, the NP/siPLK1 only remained 40% of the wound area without the modification of FA. The cell invasion ability of SGC-7901 cells after the treatment also measured by Transwell assay. In Figure 5D, the numbers of invaded cells sharply decreased after the treatment of NP/siPLK1 and NPF/siPLK1, which revealed that the silencing of PLK1 could efficiently inhibit the invasion of SGC-7901 cells. The migration and invasion ability also reported being related to the expression of Notch-1 protein, which was shown to be decreased after the silencing of PLK1 in Figure 4B.[33]

Conclusion

In summary, FA-decorated leucine-bearing PEI was successfully synthesized and applied as a gene vector for targeted delivery of siPLK1. The polymer could self-assemble to nanoparticles and showed great condensation

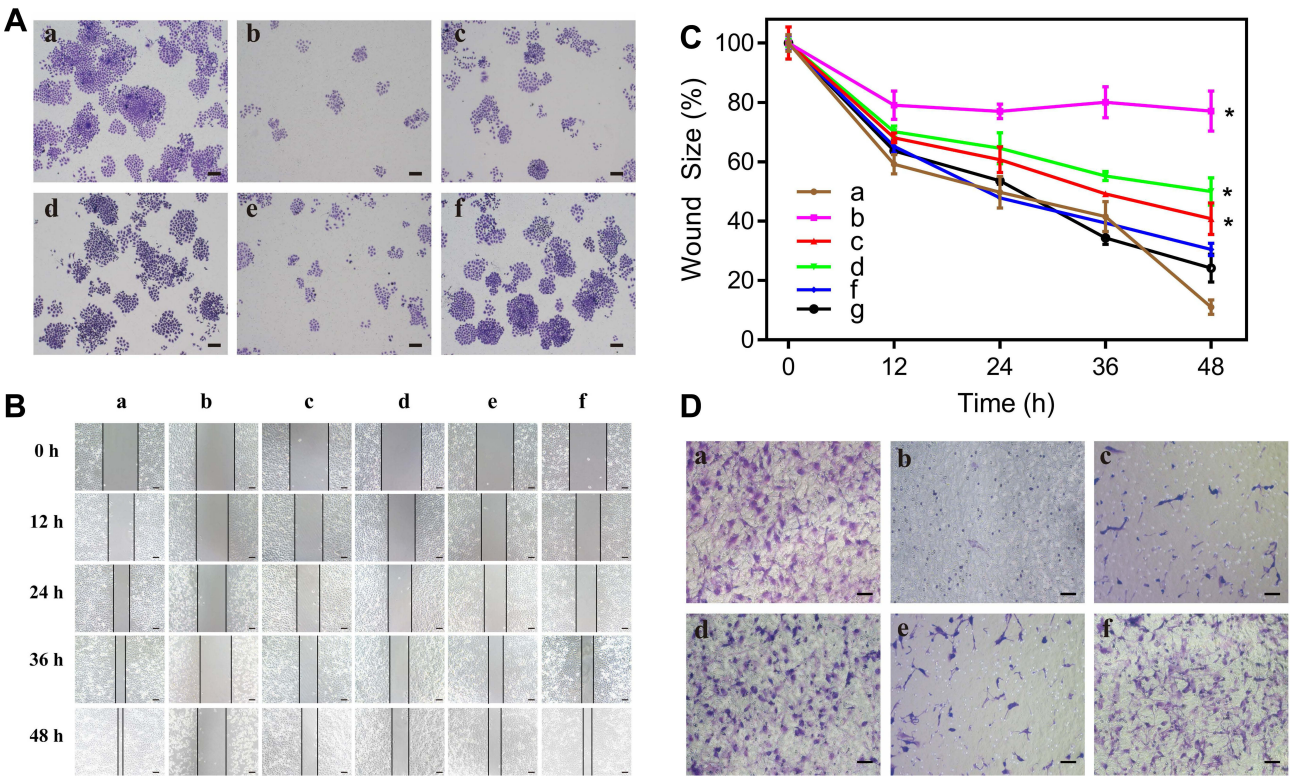

Figure 5 (**A**) Cell colony formation of SGC-7901 cells after transfection. (**B**) Wound-healing assay for evaluation of migration ability of transfected SGC-7901 cells. (**C**) Relative wound size at different time after transfection. (**D**) Transwell assay for evaluation of invasion ability of transfected SGC-7901 cells.

Notes: (a) Control; (b) PEI/siPLK1; (c) NP/siPLK1; (d) NPF/siPLK1 siRNA; (e) NPF/NC; (f) Blank NPF. The scale bar is (**A**) 200 μm, (**B**) 100 μm, (**D**) 50 μm. The data are represented as mean value ± SD of triplicate experiments (*$p < 0.05$).

Abbreviations: NP, N-acetyl- L-leucine-polyethylenimine; NPF, Folate- N-acetyl- L-leucine-polyethylenimine.

ability of siRNA. With FA modification, NPF/siPLK1 showed better cellular uptake and gene silencing in FA receptor-overexpressed SGC-7901 cell line than that in A549 cell line with a low density of FA receptor. Depletion of PLK1 induced G2 phase cell cycle arrest disturbed the mitochondrial membrane potential, and finally led to endogenous apoptosis. As predicted, incubation of NPF/siPLK1 enhanced the anti-proliferation effect, and even reduced the migration and invasion ability of SGC-7901 cell line, providing great potential in targeted delivery of siPLK1. Therefore, NPF has potential in gene delivery and gene therapy. In the future, animal experiments have been considered and will continue to be completed.

Acknowledgments

This research was funded by the Science and Technology Department of Jilin Province (Grant No. 20190201176JC), Science and Technology Department of Changchun City (Grant No.17DY018), and Education Department of Jilin Province (JJKH20180177KJ).

Disclosure

The authors report no conflicts of interest in this work.

References

1. Eckerdt F, Yuan J, Strebhardt K. Polo-like kinases and oncogenesis. *Oncogene*. 2005;24(2):267. doi:10.1038/sj.onc.1208273
2. Strebhardt K, Ullrich A. Targeting polo-like kinase 1 for cancer therapy. *Nat Rev Cancer*. 2006;6:321. doi:10.1038/nrc1841
3. Spänkuch-Schmitt B, Bereiter-Hahn Jr, Kaufmann M, Strebhardt K. Effect of RNA silencing of polo-like kinase-1 (PLK1) on apoptosis and spindle formation in human cancer cells. *J Natl Cancer Inst*. 2002;94(24):1863–1877.
4. Liu X, Erikson RL. Polo-like kinase (Plk)1 depletion induces apoptosis in cancer cells. *Proc Natl Acad Sci*. 2003;100(10):5789–5794.
5. Truong NP, Gu W, Prasadam I, et al. An influenza virus-inspired polymer system for the timed release of siRNA. *Nat Commun*. 2013;4:1902.
6. Greco KA, Franzen CA, Foreman KE, Flanigan RC, Kuo PC, Gupta GN. PLK-1 silencing in bladder cancer by siRNA delivered with exosomes. *Urology*. 2016;91(241):e241–241. e247.
7. Wang M, Alberti K, Varone A, Pouli D, Georgakoudi I, Xu Q. Enhanced intracellular siRNA delivery using bioreducible lipid-like nanoparticles. *Adv Healthc Mater*. 2014;3(9):1398–1403.
8. David S, Pitard B, Benoît J-P, Passirani C. Non-viral nanosystems for systemic siRNA delivery. *Pharmacol Res*. 2010;62(2):100–114.
9. Hartono SB, Phuoc NT, Yu M, et al. Functionalized large pore mesoporous silica nanoparticles for gene delivery featuring controlled release and co-delivery. *J Mater Chem B*. 2014;2(6):718–726.

10. Leamon CP, Low PS. Folate-mediated targeting: from diagnostics to drug and gene delivery. *Drug Discov Today*. 2001;6(1):44–51. doi:10.1016/S1359-6446(00)01594-4
11. Mattes MJ, Major PP, Goldenberg DM, Dion AS, Hutter RV, Klein KM. Patterns of antigen distribution in human carcinomas. *Cancer Res*. 1990;50(3 Supplement):880s–884s.
12. Kim SH, Jeong JH, Cho KC, Kim SW, Park TG. Target-specific gene silencing by siRNA plasmid DNA complexed with folate-modified poly (ethylenimine). *J Control Release*. 2005;104(1):223–232. doi:10.1016/j.jconrel.2005.02.006
13. Ohyama A, Higashi T, Motoyama K, Arima H. Ternary complexes of folate-PEG-appended dendrimer (G4)/α-cyclodextrin conjugate, siRNA and low-molecular-weight polysaccharide sacran as a novel tumor-selective siRNA delivery system. *Int J Biol Macromol*. 2017;99:21–28. doi:10.1016/j.ijbiomac.2017.02.045
14. Dohmen C, Fröhlich T, Lächelt U, et al. Defined folate-PEG-siRNA conjugates for receptor-specific gene silencing. *Mol Ther Nucl Acids*. 2012;1:e7. doi:10.1038/mtna.2011.10
15. Tian H, Xiong W, Wei J, et al. Gene transfection of hyperbranched PEI grafted by hydrophobic amino acid segment PBLG. *Biomaterials*. 2007;28(18):2899–2907. doi:10.1016/j.biomaterials.2007.02.027
16. Aldawsari H, Raj BS, Edrada-Ebel R, et al. Enhanced gene expression in tumors after intravenous administration of arginine-, lysine-and leucine-bearing polyethylenimine polyplex. *Nanomedicine*. 2011;7 (5):615–623. doi:10.1016/j.nano.2011.01.016
17. Ewe A, Przybylski S, Burkhardt J, Janke A, Appelhans D, Aigner A. A novel tyrosine-modified low molecular weight polyethylenimine (P10Y) for efficient siRNA delivery in vitro and in vivo. *J Control Release*. 2016;230:13–25. doi:10.1016/j.jconrel.2016.03.034
18. Ewe A, Höbel S, Heine C, et al. Optimized polyethylenimine (PEI)-based nanoparticles for siRNA delivery, analyzed in vitro and in an ex vivo tumor tissue slice culture model. *Drug Deliv Transl Res*. 2017;7(2):206–216. doi:10.1007/s13346-016-0306-y
19. Xia J, Chen L, Chen J, et al. Hydrophobic polyphenylalanine-grafted hyperbranched polyethylenimine and its in vitro gene transfection. *Macromol Biosci*. 2011;11(2):211–218. doi:10.1002/mabi.v11.2
20. Fu C, Lin L, Shi H, et al. Hydrophobic poly (amino acid) modified PEI mediated delivery of rev-casp-3 for cancer therapy. *Biomaterials*. 2012;33(18):4589–4596.
21. Xing Z, Gao S, Duan Y, et al. Delivery of DNAzyme targeting aurora kinase A to inhibit the proliferation and migration of human prostate cancer. *Int J Nanomedicine*. 2015;10:5715–5727.
22. Song Z, Liang X, Wang Y, et al. Phenylboronic acid-functionalized polyamidoamine-mediated miR-34a delivery for the treatment of gastric cancer. *Biomater Sci*. 2019;7(4):1632–1642.
23. Li Z, Zhang L, Li Q. Induction of apoptosis in cancer cells through N-acetyl-l-leucine-modified polyethylenimine-mediated p53 gene delivery. *Colloids Surf B Biointerfaces*. 2015;135:630–638.
24. Weerdt B, Medema RH. Polo-like kinases: a team in control of the division. *Cell Cycle*. 2006;5(8):853–864.
25. Wu ZY, Wei N. Knockdown of PLK1 inhibits invasion and promotes apoptosis in glioma cells through regulating autophagy. *Eur Rev Med Pharmacol Sci*. 2018;22(9):2723–2733.
26. Mao Y, Xi L, Li Q, et al. Regulation of cell apoptosis and proliferation in pancreatic cancer through PI3K/Akt pathway via Polo-like kinase 1. *Oncol Rep*. 2016;36(1):49–56.
27. Sekimoto N, Suzuki Y, Sugano S. Decreased KPNB1 Expression is Induced by PLK1 Inhibition and Leads to Apoptosis in Lung Adenocarcinoma. *J Cancer*. 2017;8(19):4125–4140.
28. Tournier C, Hess P, Yang DD, et al. Requirement of JNK for stress-induced activation of the cytochrome c-mediated death pathway. *Science*. 2000;288(5467):870–874.
29. Wang J, Kho D, Zhou J-Y, Davis RJ, Wu GS. MKP-1 suppresses PARP-1 degradation to mediate cisplatin resistance. *Oncogene*. 2017;36(43):5939.
30. Chen X-B, Li W, Chu A-X. MicroRNA-133a inhibits gastric cancer cells growth, migration, and epithelial-mesenchymal transition process by targeting presenilin 1. *J Cell Biochem*. 2019;120(1):470–480.
31. Franken NA, Rodermond HM, Stap J, Haveman J, van Bree C. Clonogenic assay of cells in vitro. *Nat Protoc*. 2006;1(5):2315–2319.
32. Chen J, Ding J, Xu W, et al. Receptor and microenvironment dual-recognizable nanogel for targeted chemotherapy of highly metastatic malignancy. *Nano Lett*. 2017;17(7):4526–4533.
33. Bu P, Chen K-Y, Chen Joyce H, et al. A microRNA miR-34a-regulated bimodal switch targets notch in colon cancer stem cells. *Cell Stem Cell*. 2013;12(5):602–615.